ANNUAL REVIEWS

Annual Review of Genomics and Human Genetics

Extrachromosomal DNA in Cancer

Vineet Bafna[1] and Paul S. Mischel[2]

[1]Department of Computer Science and Engineering and Halıcıoğlu Data Science Institute, University of California, San Diego, La Jolla, California, USA; email: vbafna@cs.ucsd.edu

[2]Department of Pathology and ChEM-H, Stanford University School of Medicine, Stanford, California, USA; email: pmischel@stanford.edu

Annu. Rev. Genom. Hum. Genet. 2022. 23:29–52

First published as a Review in Advance on May 24, 2022

The *Annual Review of Genomics and Human Genetics* is online at genom.annualreviews.org

https://doi.org/10.1146/annurev-genom-120821-100535

Keywords

ecDNA, cancer, homogeneously staining regions, HSRs, ecDNA evolution, ecDNA hubs, enhancer hijacking

Abstract

In cancer, complex genome rearrangements and other structural alterations, including the amplification of oncogenes on circular extrachromosomal DNA (ecDNA) elements, drive the formation and progression of tumors. ecDNA is a particularly challenging structural alteration. By untethering oncogenes from chromosomal constraints, it elevates oncogene copy number, drives intratumoral genetic heterogeneity, promotes rapid tumor evolution, and results in treatment resistance. The profound changes in DNA shape and nuclear architecture generated by ecDNA alter the transcriptional landscape of tumors by catalyzing new types of regulatory interactions that do not occur on chromosomes. The current suite of tools for interrogating cancer genomes is well suited for deciphering sequence but has limited ability to resolve the complex changes in DNA structure and dynamics that ecDNA generates. Here, we review the challenges of resolving ecDNA form and function and discuss the emerging tool kit for deciphering ecDNA architecture and spatial organization, including what has been learned to date about how this dramatic change in shape alters tumor development, progression, and drug resistance.

1. INTRODUCTION, DISCOVERY, AND NOMENCLATURE

Eukaryotic circular chromosomal structures have been part of the vernacular of genetics since its early days. In 1932, McClintock (67) discovered the presence of ring-shaped chromosomes in maize and observed that "a deletion in the short arm of the bm_1 chromosome comparable in extent to the most frequently observed size of the ring chromosome was also present. . . . The ring chromosome did not synapse with the homologous region in the normal chromosome" (p. 679). The notions of chromosomal deletion, circularization, acentricity, and independent segregation—hallmarks of extrachromosomal circular DNA (eccDNA) formation—are all implicit in these prescient remarks. Nevertheless, it was another three decades before circular DNA structures were predicted in plants (wheat nuclei) and animals (boars) based on their biochemical similarity to *Escherichia coli* (34). In 1965, two publications definitively documented larger extrachromosomal DNA (ecDNA) through direct observation of cells: First, Cox et al. (19) observed minute chromatin bodies in neuroblastoma cells during metaphase, where they often appeared paired as double minutes (DMs), and second, Lubs & Salmon (57) observed aberrantly sized deleted chromosomes that were distinct from the rod-shaped, condensed chromosomes typically seen in metaphase. Subsequent research often used the term DMs, but also the terms double fragments of chromosomes, double bodies, and accessory chromatin, to describe these extrachromosomal structures.

We use the term eccDNA to encompass all acentric (not containing a centromere), circular DNA structures in eukaryotic cells. We contrast eccDNA with other large chromosomal fragments that have circularized to form ring chromosomes or neochromosomes and are often seen in highly rearranged tumor genomes (27). Specifically, ring chromosomes have centromeres (66), including ectopic centromeres (115, 116), while eccDNA is acentric. eccDNA can be further classified based on size. Smaller elements ($<10^4$ base pairs) appear to be abundant in all cells (34, 48, 117), sometimes express noncoding RNA capable of affecting gene expression (48, 82, 83), and have recently been shown to be immunostimulatory (117). We refer to these elements as microDNA. Ring chromosomes and microDNA are not discussed further in this review. Instead, we focus on larger (10^4–10^7 base pairs), acentric, circular molecules that are typically visible in an optical microscopy image. While there is some debate about terminology, we refer to these molecules as ecDNA to emphasize that they are found not only as pairs (DMs) but also as singletons and as aggregated hubs (as discussed further below) (36), that they are derived largely from chromosomal DNA but exist outside of it, and that their acentricity and extrachromosomality govern much of their (dys)function.

2. FOUNDATIONAL EXPERIMENTS

The initial discoveries of ecDNA were quickly recapitulated in many other contexts, usually in cancer cells (47, 64, 71, 90, 98). Despite repeated observations of ecDNA, very basic questions regarding how ecDNA molecules replicate and segregate into daughter cells upon mitosis remained technically difficult to resolve, at least partly because ecDNAs could only be reliably observed during metaphase, when the chromosomes are compacted and ecDNAs can be directly observed as distinct chromatin bodies. The discovery of cultured mouse cells in which the ecDNAs were large and distinctive enough to be observed during anaphase resolved some of these issues. Levan & Levan (53) concluded, based on the orientation and positioning of chromosomes and ecDNAs, that ecDNAs did not orient with the rest of the chromosomes; instead of being directly pulled by spindle fibers, they were either tethered to chromosomal ends or clustered in peripheral nucleolar regions. The authors also observed anaphase bridge formation, with beads of ecDNA strung out along the bridge. Together, these results established the acentricity of ecDNA.

Despite the lack of spindle attachments, ecDNA transmission into daughter cells was efficient; ecDNAs were tethered to chromosomes, so they remained inside the nucleus upon cell division and were not lost into the cytosol and degraded. These events were subsequently demonstrated and confirmed in live cells (40). Barker et al. (7) and Takayama & Uwaike (105) later used BrdU labeling experiments to show that ecDNAs were capable of replicating independently and at the same rate as chromosomal DNA. Independently, and much later, their segregation into daughter cells was shown to be random and approximately Gaussian (as a limiting process of the binomial distribution) (51, 59). Another line of research suggested the circularity, or at least nonlinearity, of ecDNA in murine cell lines (32), an idea that was subsequently and beautifully confirmed with high-resolution scanning electron microscopy images overlaid on 4′,6-diamidino-2-phenylindole (DAPI)–stained metaphase images of cancer cells (118).

A series of remarkable papers coming out of the Schimke laboratory provided a foundation for ecDNA exploration. In studying a murine cancer cell line that had achieved resistance to methotrexate, Alt et al. (4) found a huge amplification of the dihydrofolate reductase gene (*DHFR*). The *DHFR* copy number amplification and resistance were both lost upon drug removal. The unstable amplification was due to ecDNA formation. However, a different cell line showed a stable resistance phenotype and consistent but lower *DHFR* amplification, which was subsequently attributed to *DHFR* aggregation and integration in a chromosomal location to form a homogeneously staining region (HSR) (41). HSRs had previously been observed along with ecDNA in neuroblastoma cell lines, where it was suggested that the HSRs were excised to form ecDNA (6). However, observations of the COLO320 colorectal cancer cell line across many passages reversed this conclusion. COLO320 cells originally carried ecDNA containing the oncogene *c-Myc*, but across many passages, a majority of the cells showed *c-Myc* to be integrated into a chromosomal location as HSRs (3), suggesting that ecDNAs arose before HSRs. The ecDNA and HSR mechanisms of amplification were directly correlated in an elegant experiment where continuous growth of the cell line over many passages under methotrexate treatment led to the *DHFR* gene being incorporated stably into the chromosome (8, 42).

While eccDNAs were observed in normal or nonstressed cells in other contexts (34), including animals and plants, they appeared to be mostly microDNAs, not ecDNAs (48). MicroDNA is indeed abundant in human and other cells (73). There was also a suggestion early on that smaller, episomal structures could recombine into larger ecDNAs (13), but even the episomes (size 10^5 base pairs) were still larger than typical microDNA. Moreover, other experiments suggested that ecDNA formation was a rare event and not adequately explained by recombination from smaller circular microDNA (31). Until further evidence is revealed in support of a common origin, we can assume that microDNA and ecDNA are unrelated phenomena.

In fact, most of the early ecDNA observations were obtained in cancer cells. The ecDNAs were large enough to carry genes, and many were found to amplify the copy number and activity of newly discovered oncogenes, including *c-Myc* (3) and *n-Myc* (45), which could provide a proliferative advantage over the cells. Other observations of ecDNA came from cells that were stressed in a manner that provided a fitness advantage to ecDNA carriers (8, 41, 42). Notably, ecDNA-carrying cells often lost them efficiently in the absence of selective pressure from drug treatment (4, 10) or simply in transference from mouse xenografts to cell cultures (42). These observations remain relevant today. With technological improvements allowing for the testing of ecDNA presence in thousands of samples, ecDNAs have rarely been observed in normal tissue from cancer patients even when the tumor cells of those patients have abundant ecDNA (43, 107). Large ecDNAs have been observed in plants (weeds), but, once again, they function as a pesticide resistance mechanism (46, 72).

Thus, while not apparent at the time, a retrospective reading of these papers in combination with new results seems to confirm that, unlike microDNA formation, ecDNA formation is a rare event, and its continued maintenance is unique to cells in which ecDNAs provide a fitness advantage.

3. TOWARD A MODEL OF EXTRACHROMOSOMAL DNA EVOLUTION

The results from the foundational experiments can be distilled to support a working model of ecDNA evolution, which we propose here as a starting point (albeit one that is not widely accepted and will almost certainly be revised in the future):

1. ecDNAs form in a stochastic event that involves double-strand breaks in the linear chromosome, followed by ligation to circularize the unprotected ends (see Section 5).
2. ecDNAs replicate independently at rates similar to those of linear chromosomes (7).
3. The replicated ecDNAs segregate at random into the daughter cells (51, 59).
4. The cellular microenvironment imposes a selection bias for ecDNA-carrying cells, which has direct implications for the continued presence of ecDNAs or their elimination from the population (4, 41, 42, 51).

These observations were recently put into a mathematical model and investigated systematically by Lange et al. (51) (also see **Figure 1**). Consider a scenario where a single ecDNA is generated, and denote that time as $t = 0$. Each subsequent mitosis doubles the number of cells. Let $N_k(t)$ describe the number of cells with exactly k ecDNAs at time t of a population of $N(t) = \sum_{k=0}^{\infty} N_k(t)$ cells. Consider one of the $N_i(t)$ cells carrying i copies of ecDNA. The ecDNAs self-replicate to form $2i$ ecDNA copies prior to mitosis. Random segregation leads to the two daughter cells obtaining k and $2i - k$ ecDNA copies according to the binomial distribution for all $0 \le k \le 2i$. Evolving values of $N_k(t)$ (the distribution of ecDNA counts among cells) are governed by the following system of coupled differential equations:

$$\frac{\mathrm{d}N_k(t)}{\mathrm{d}t} = -sN_k(t) + 2s \sum_{i=\lceil \frac{k}{2} \rceil}^{\infty} N_i(t) \binom{2i}{k} \frac{1}{2^{2i}}, \quad 1.$$

$$\frac{\mathrm{d}N_0(t)}{\mathrm{d}t} = N_0(t) + 2s \sum_{i=1}^{\infty} N_i(t) \frac{1}{2^{2i}}. \quad 2.$$

Here, s denotes a selection coefficient such that ecDNA-carrying cells are s-fold more likely to divide than noncarriers. Carriers have a fitness advantage when $s > 1$, have a disadvantage when $s < 1$, and are neutral when $s = 1$. While the coupled nature of the equations makes it difficult to solve them analytically, simulations allow us to model many aspects of ecDNA.

Simulations of the model showed that in the absence of selection ($s = 1$) or with negative selection ($s < 1$), the fraction of cells carrying ecDNA [$1 - N_0(t)/N(t)$] rapidly decays, completely consistent with ecDNA not being observed in normal cells (51). On the flip side, $N_0(t)/N(t)$ approaches 0 in simulations with positive selection, even for a small selective advantage. These complementary results suggest that the presence of ecDNA should coincide with the presence of a functional element that confers a selective advantage. We explore this facet further in Section 6.

The model also makes a direct prediction of the distribution of ecDNA in cells, with the tail probabilities suggesting a distribution that is wider than the normal distribution but somewhat narrower than an exponentially decaying distribution [$e^{-\lambda x^2} \le \Pr(N_k(t)/N(t) = x) \le e^{-\lambda x}$ for large x]. The model predictions were nicely validated when they were compared against experimentally observed ecDNA distributions in multiple cell lines and s was chosen to best fit the experimental

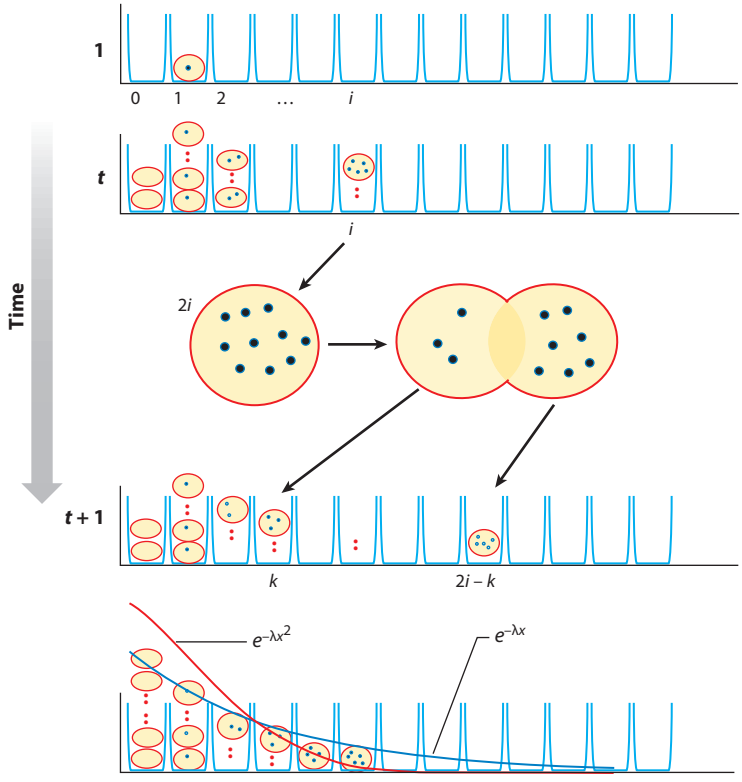

Figure 1

A model of ecDNA evolution. Bin i maintains the count $N_i(t)$ of the number of cells with exactly $i \geq 0$ ecDNA copies. At $t = 1$, $N_1(1) = 1$ and all other bins are 0. An ecDNA-positive cell is s times more likely to be picked than an ecDNA-negative cell, where s denotes the selection coefficient. The chosen cell with i ecDNA copies replicates and divides into two daughter cells containing k and $2i - k$ ecDNAs, chosen according to a binomial distribution. Simulations suggest that in the absence of selection ($s = 1$) or with negative selection ($s < 1$), the proportion of ecDNA-negative cells in the population increases to 1, but for $s > 1$, this proportion rapidly diminishes. In the limit, the tail distribution of ecDNA counts is wider than the normal distribution but somewhat narrower than an exponentially decaying distribution. Abbreviation: ecDNA, extrachromosomal DNA.

data (51). The results showed a good fit to the simulation-based predictions of ecDNA count distribution and clearly indicated that ecDNAs were under positive selection. The results also explained the relatively high heterogeneity of ecDNA copy number. Finally, with modest positive selection, the typical number of ecDNAs per cell remains in the hundreds.

Nevertheless, the model is simplistic in its treatment of selection, in that the fitness advantage depends solely on the presence or absence of ecDNAs and not on their abundance. It also does not account for the loss of ecDNAs. Other models have worked with more complex selection regimes where the fitness is reduced with increasing ecDNA due to additional metabolic load (107). With improved experimentation methods, the models could be refined to make precise, quantitative predictions of the fitness advantage of ecDNA formation and provide a foundation for exploring ecDNA evolution.

Even in its current simple form, the model provides a useful framework for studying ecDNA. The remainder of this review attempts to explain the experimental data using the model-based

framework, and we also refine the model as we go along. Specifically, we discuss how ecDNAs form, how prevalent they are in cancer or normal cells, the exact mechanisms of random segregation, what functional properties lead to positive selection, how they correlate with increased cancer pathology, how these functional aspects could be co-opted for intervention and therapy, and the mechanisms by which ecDNAs are lost under negative selection or simply the absence of positive selection. Before we address these points, however, we consider a technical detour aimed at reliably detecting ecDNA.

4. IDENTIFYING EXTRACHROMOSOMAL DNA AND ELUCIDATING ITS PRIMARY STRUCTURE

4.1. Cytogenetic Methods for Detecting Extrachromosomal DNA

During metaphase, the chromosomes are compacted and aligned on the metaphase plate, making it easier to identify ecDNAs as distinct structures after staining DNA with DAPI. Metaphase DAPI continues to be one of the most reliable methods of ecDNA discovery, but until recently it was a low-throughput method. Turner et al. (107) used automated computer-vision-based methods to count the number of ecDNAs per cell across a multitude of cells with high specificity (few false ecDNA calls) but somewhat lower sensitivity. Recent advances in deep neural networks have led to the development of fully convolutional neural networks for the problem of image segmentation (56), where the objective is to reliably assign a category or label to each pixel of the image. In an application of these ideas to metaphase images, Rajkumar et al. (85) trained a convolutional neural network with the u-net architecture to assign each pixel of a DAPI image to one of four categories: ecDNA, cytoplasm, chromosome, or intact nucleus. The trained networks could identify ecDNA pixels with close to 85% accuracy, even when the ecDNA contours were proximal to chromosomes and not easily distinguished with computer-vision methods. The utilization of these methods helped identify ecDNA at scale in thousands of images and provided reliable estimates of the prevalence of ecDNA.

Recall from the model represented by Equations 1 and 2 that the high heterogeneity and wide tail of ecDNA distribution demands the sampling of a larger number of cells (20–200) for accurate estimates. The classification of a sample as ecDNA positive is determined by somewhat arbitrary but reasonable cutoffs of $\geq$2 ecDNAs per cell (107) or a more aggressive measure of 1 ecDNA for every 2 cells on average, with at least 20 cells sampled (43). The estimation of ecDNA distribution has allowed for a precise calculation of the impact (selection strength) of drug treatment by measuring the change in ecDNA distribution (51, 85, 118).

While highly accurate, DAPI staining is not sufficient to resolve the different ecDNA forms that a cell may present. DAPI signals cannot be detected for microDNA, and very small ecDNAs ($\sim 10^5$ base pairs) may also be missed. The use of fluorescence in situ hybridization (FISH) using specific DNA probes allows for the positioning of specific genomic regions inside or outside of chromosomes and has revealed cells with small (<100 kb) ecDNA (22). It has also resolved the counts and copy numbers of multiple distinct ecDNA structures, each amplifying a different gene (36). DNA FISH requires prior knowledge of the probes and is typically used in conjunction with a DNA copy number analysis method to identify probes in genomic regions with focal copy number amplification.

Metaphase analysis requires growing cells, which are often not available from primary cancer tissues. DNA FISH and other hybridization methods have been used to validate the genomic content of ecDNA and to study the amplification of specific DNA regions directly from interphase cells. The reliable identification of ecDNA in interphase cells remains an unsolved problem.

4.2. Next-Generation Sequencing for Extrachromosomal DNA Identification and Structure

The genomics revolution, starting with the sequencing and assembly of the human genome (38, 110) and followed by the development of massively parallel paired-end next-generation sequencing and subsequent paired-end mapping of query DNA from donor samples, allowed for the fine mapping of both small nucleotide variants and larger structural variants in the donor genome (88, 108, 121). While revolutionary, the Human Genome Project "sucked a lot of the oxygen out of the room" (20), which included an impact on ecDNA research. The early genomics projects focused more on detecting smaller single-nucleotide variation or simpler structural variation in the form of measuring copy number changes and translocation events, which were the easiest to discover using genomic short reads. While aneuploidies and copy number amplifications were identified and treated as events with consequences, particularly in cancer, their spatial relationships and mechanistic aspects were set aside or forgotten.

Methods for paired-end next-generation-sequencing-based mapping (54) and structural variant identification began to be used to identify the structural features of ecDNA (**Figure 2*a***) and HSRs from cancer cell lines (49, 89, 103, 104) and xenografted tumor cells (111). These methods have recently been extended and refined to automatically elucidate the genomic structure, or architecture, of ecDNA from whole-genome sequencing data (22, 107, 119). The computational problem is related to de novo genome assembly but is distinct. First, unlike chromosomes, which are typically diploid, ecDNAs appear in multiple copies per cell and may have significant structural heterogeneity. Second, in de novo genome assembly, there is no prior knowledge of the primary sequence, and the assembled sequence must be generated by stitching overlapping fragments together. On the other hand, as the ecDNA segments are all derived from chromosomal segments from a known genomic reference, the fragments can be mapped to the reference first to identify distinct genomic regions mapping ecDNA (**Figure 2*b***). Moreover, paired-end or split reads with ends mapping to distinct genomic segments describe breakpoints that help stitch those segments together in the correct orientation to elucidate the genomic structure of ecDNA. Several methods have therefore adapted this technique of directed assembly to determine the structure of ecDNA and other focal amplicons (22, 89, 92, 119). Other graph- and string-based explorations of complex genomic rearrangements that include but are not focused on ecDNA are also becoming an essential part of the genomic tool kit (12, 30).

The AmpliconArchitect method starts by identifying seed regions of focal amplification and explores breakpoints that connect these regions to other distinct regions. It next builds a graph where nodes correspond to the ends of segments. Edges represent either segments or breakpoints connecting two distinct segments through deletion, inversion, or translocation. The resulting amplicon graph is a compact representation of all possible structures encoding the focal amplification (**Figure 2*c***). Circular paths in the graph represent putative ecDNA structures, and in many cases a single (cyclic) path explains most of the copy number amplification of the genome, providing an unambiguous ecDNA structure. For complex, heterogeneous ecDNA structures, short reads may not suffice to provide a unique structure, especially when a large segment is repeated multiple times in the ecDNA. For instance, an amplicon graph constructed using short reads sampled from the ecDNA in **Figure 2*a*** permits multiple ecDNA structures (**Figure 2*d***).

Even in the absence of unique structure reconstruction, the amplicon graph provides a powerful abstraction of the amplicon structure, because it identifies the (possibly multichromosomal) genomic intervals that are part of the ecDNA (**Figure 2*b*,*c***). Integration of functional information, including chromatin accessibility, gene expression, chromatin conformation, and DNA interactions, into the amplicon graphs can reveal important functional aspects of ecDNA (see Section 6).

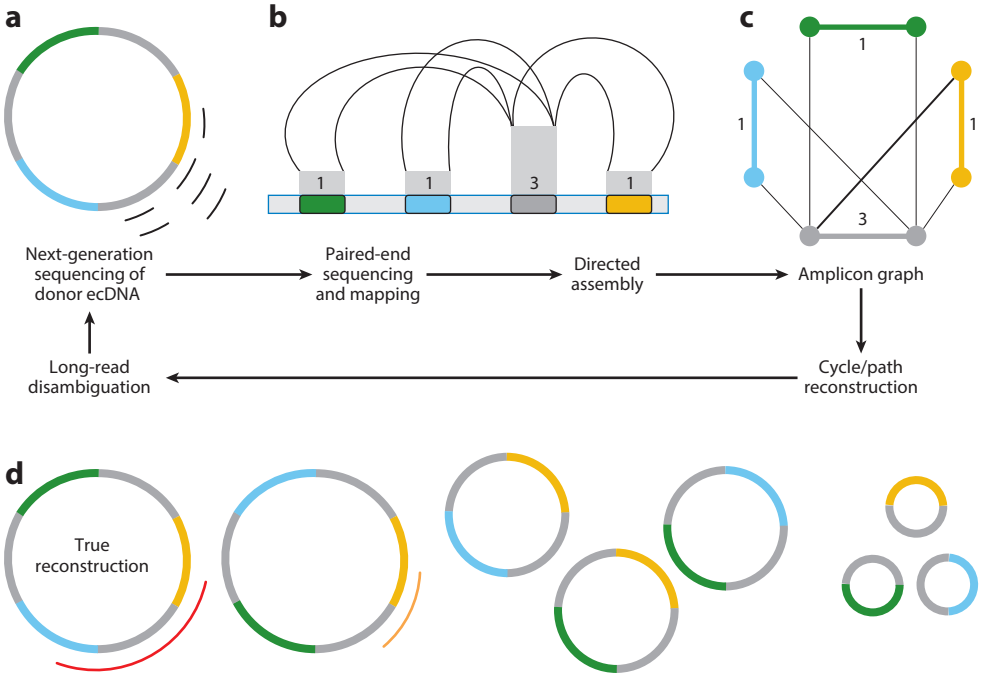

Figure 2

Directed assembly for ecDNA structure and detection. (*a*) Short reads from whole-genome sequencing also sample ecDNA structures. (*b*) Paired-end sequencing and mapping identify breakpoints and copy number changes. The colored segments represent genomic intervals of an amplicon, the gray boxes represent estimates of the copy number and multiplicities of segments (*numbers*), and the thin black lines represent breakpoints connecting the segments. (*c*) Directed assembly methods smooth out the coverage and generate an amplicon graph representing all amplified segments and their multiplicities and breakpoints. (*d*) Paths and cycles in the amplicon graph help detect ecDNAs (e.g., long, high-copy cycles) and their fine structure. Large segments with high multiplicities (*gray segments*), missing breakpoints, or heterogeneity of ecDNA all lead to ambiguity of reconstruction. All cycles in this panel are consistent with the breakpoint graph. Long reads help detect breakpoints that short reads may have missed due to the low complexity of the sequence. Long reads that span high-multiplicity regions resolve ambiguities in reconstruction. The far left circle represents the true reconstruction. Abbreviation: ecDNA, extrachromosomal DNA.

While genomic analysis is used primarily to understand the fine structure of ecDNA, it could also be utilized to predict the presence of ecDNA based on the presence or absence of high-copy cycles in the amplicon graph (22, 43, 119). This argument needs some clarification because repeated tandem duplications could also mechanistically explain cycles in the amplicon graph. However, that explanation is contingent on the reuse of identical breakpoints multiple times—an unlikely event. Kim et al. (43) compared genomic and cytogenetic data to show that amplicon analysis could indeed predict ecDNA with high sensitivity and specificity (>82% for both). In fact, because ecDNA is functionally different from chromosomal DNA (see Section 6), recent research has also utilized functional data—specifically, data from the assay for transposase-accessible chromatin with high-throughput sequencing (ATAC-seq)—to detect microDNA and ecDNA (48, 74), and future work is likely to incorporate other sources of functional data to reliably detect ecDNA in bulk and single-cell modes (16, 33, 118).

Despite these developments, ecDNA identification using short reads has its challenges. ecDNAs reintegrate into chromosomes in nonnative locations as HSRs. The integration often

involves multiple copies of an ecDNA and preserves its fine structure, making it difficult to distinguish between ecDNAs and HSRs. Koche et al. (44) observed a palm-tree motif, with the fronds indicative of chromosomal integration of ecDNAs (HSRs). The palm-tree signal could be used to distinguish ecDNAs from HSRs but may not be visible when the integration happens at few (perhaps one or two) locations. With short-read sequencing, it is hard to detect pure ecDNA in hybrid ecDNA and HSR structures. At the same time, much research (36, 42, 77, 101, 104) suggests that the movement between ecDNAs and HSRs is dynamic and that cell populations carrying both ecDNAs and HSRs coexist (8, 37), diminishing the need for a strict differentiation between these two states. A second challenge with short-read sequencing is that cyclic structures may be detected, with multiple fold-back discordant reads connecting duplicated segments head to head or tail to tail arising due to breakage–fusion–bridge (BFB) cycles (see Section 5). Conservatively, signatures of BFB (124) are used to preclude ecDNA calls prior to calling ecDNA (43).

4.3. Some Long Reads Are More Equal than Others

Breakpoints that lie in repetitive or low-complexity sequence at breakpoint junctions are often missed by short reads, which accounts for most of the false negatives in short-read-based ecDNA identification (43). Additionally, the presence of repetitive sequence leads to ambiguous paths in the amplicon graph. It has long been a mantra that long reads can help disambiguate complex assembly (or amplicon) graphs. Disambiguation can be achieved by reads that can span the entire repetitive region. For instance, the amplicon graph in **Figure 2*c*** supports many possible reconstructions obtained by traversing cycles (**Figure 2*d***). However, the presence of a single long read is sufficient to select the one true cycle as long as it spans the region of high multiplicity (**Figure 2*d***). Technologies such as nanopore sequencing and the Pacific Biosciences Single Molecule, Real-Time (SMRT) and HiFi sequencing platforms generate reads that are long enough to span most common repeats in the human genome [where long interspersed nuclear elements (LINEs) are approximately 10 kb]; these technologies can therefore theoretically identify all breakpoints of an amplicon, and they are being increasingly utilized for ecDNA analysis (22, 33). However, these technologies typically have a limited yield for DNA fragment sizes in excess of 40–50 kb. Single-molecule sequencing allows for the direct measurement of DNA methylation without the need for bisulfite conversion and has been used to elucidate ecDNA function (33). However, the current yields of very long reads (>200 kb) for this technology are also low. Therefore, large duplicated regions seen in ecDNA may not be spanned, making it difficult to resolve all ambiguities.

Optical mapping is emerging as another technology of interest for investigating structural variants in cancer genomes (39). This technology is derived from one of the early innovations of genomics, where restriction-fragment-based physical mapping of clones allowed for the identification of a clone and its overlapping partners without sequencing (23). In its new incarnation, isolated DNA molecules of up to 250 kb are at first stretched out in nanochannels. Next, specific motifs on the molecules are recognized and fluorescence imaged to provide optical restriction maps for each molecule (50). The intermarker distances can be used to detect overlapping fragments and assemble very large molecules (>1 Mb) of restriction-site locations. These contigs can be analyzed using specialized algorithms to identify structural variation (52, 58, 84) and have been used in conjunction with next-generation sequencing to successfully disambiguate ecDNA structures (16, 58, 101) (**Figure 2*d***). They have also been utilized to successfully reconstruct the architecture of large HSRs and BFB cycles and to distinguish other forms of focal amplification from ecDNA (58, 101).

4.4. Purification Before Sequencing

In Circle-seq, total genomic DNA, including ecDNA, is immobilized in a gel and digested with an exonuclease for digesting linear DNA and enriching for ecDNA (76). The enrichment is followed by rolling circle amplification to amplify the circular DNA. Subsequent sequencing with short and long reads provides a clear guide to the ecDNA segments of the genome (33). This technique works even in single cells and promises to be a great tool in tracking ecDNA heterogeneity across populations, especially in conjunction with long-read sequencing (44). It has been particularly successful for microDNA.

Some challenges remain for the larger ecDNA molecules: Inefficient exonuclease digestion may result in a lack of targeted sequence; multiple, distinct ecDNA segments can be identified but may be difficult to separate; and the rolling circle amplification may not amplify the entire ecDNA region. Some of these issues have been addressed using CRISPR-Cas9-assisted targeting of chromosome segments (CRISPR-CATCH) (35). Strategically guided CRISPR-based cuts linearize small ecDNA-derived segments that can be separated from the larger chromosomal segments and from heterogeneous ecDNA using pulsed-field gel electrophoresis. Next-generation sequencing of gel bands followed by customized algorithmic analysis leads to simpler amplicon graphs with unique cyclic paths. Moreover, different bands and CRISPR guides provide a structural determination of ecDNA heterogeneity and can elucidate the structures of multiple distinct ecDNAs in one sample.

Overall, the tremendous growth of technologies for ecDNA detection has made it possible to estimate the prevalence of ecDNA in cancers and systematically explore its structure and function, which had long been a matter of some debate.

4.5. Estimating Extrachromosomal DNA Prevalence

The prevalence of ecDNA has also been a matter of some debate. A survey of 9,500 metaphase cells obtained from individuals with hereditary cancers, individuals with nonfamilial cancers, and controls with no tumors identified ecDNA in only 15 images, almost exclusively in patients with multiple endocrine neoplasia (90). An estimate based on surveying the Mitelman Database of Chromosome Aberrations and Gene Fusions in Cancer suggested that 1.5% of all cancer samples carried ecDNA (24). In more recent work, Turner et al. (107) utilized automated image analysis to investigate more than 2,500 cancer and normal cell lines in metaphase stained with DAPI, representing multiple tumor subtypes, and found that nearly 40% of all samples carried ecDNA. Kim et al. (43) analyzed whole-genome sequencing data from 3,212 tumors and 1,810 nonneoplastic samples and found that 460 (14.3%) of the tumor samples carried ecDNA, with no occurrence of ecDNA in normal samples. ecDNAs are abundant in other cancers, including glioma (21), neuroblastoma (33), medulloblastoma (16), and oropharyngeal cancer (81). Anecdotal evidence suggests that ecDNAs arise early in tumor development and that the frequency of ecDNA increases with the progression of the tumor, but these ideas will need to be confirmed with systematic time course analyses of tumor progression. As technologies for ecDNA detection continue to improve, these estimates will be revised, but it is likely that ecDNA occurrence is a common, pan-cancer phenomenon.

5. FORMATION OF EXTRACHROMOSOMAL DNA

5.1. Episome Formation

The most direct model of ecDNA formation is the episomal model, which involves double-strand breaks followed by religation. Carroll et al. (13) investigated an experimental model of a Chinese hamster ovary cell line with an integrated *CAD* gene array and demonstrated the formation of

ecDNA using Southern blotting methods. They posited that the episomes are usually smaller (approximately 250 kb) but gradually enlarge to become ecDNAs. They also showed that the ecDNA formation was concurrent with a deletion scar on the chromosome. Their results were generally consistent with independent observations of ecDNA formation (8, 42, 113).

Subsequently, Vogt et al. (112) used quantitative PCR and chromosome walking methods to elucidate the genetic content and ecDNA architecture in seven gliomas. This structural analysis confirmed that the ecDNA was most likely formed by a circularization of a chromosome fragment. In later work, Vogt et al. (111) showed that ecDNA fragments in gliomas overlapped the epidermal growth factor receptor (*EGFR*) gene, providing a selective advantage. However, they also observed that the corresponding chromosomal loci were not rearranged, and the presence of ecDNA did not, in fact, coincide with a corresponding deletion in any of the glioma samples. These results strongly suggested that a rereplicative or postreplicative event was responsible for the formation of each of the initial amplicons (**Figure 3*a***). For example, in the case of four copies of the chromosome (two sister-chromatid pairs), the ecDNA could cosegregate with intact chromosomes during mitosis, or sister-chromatid repair could repair the chromosomal lesion. Alternatively, in a replication bubble model, an ecDNA might excise out of a replication fork and circularize. Meanwhile, fork regression and rereplication from flanking forks would lead to sister chromatids with no scars.

Subsequent experiments analyzing the fine sequence of multiple ecDNA and HSR structures were consistent with the episome model as the basis of ecDNA formation (103, 104). Those experiments also failed to identify a corresponding deletion scar in the chromosome that matched

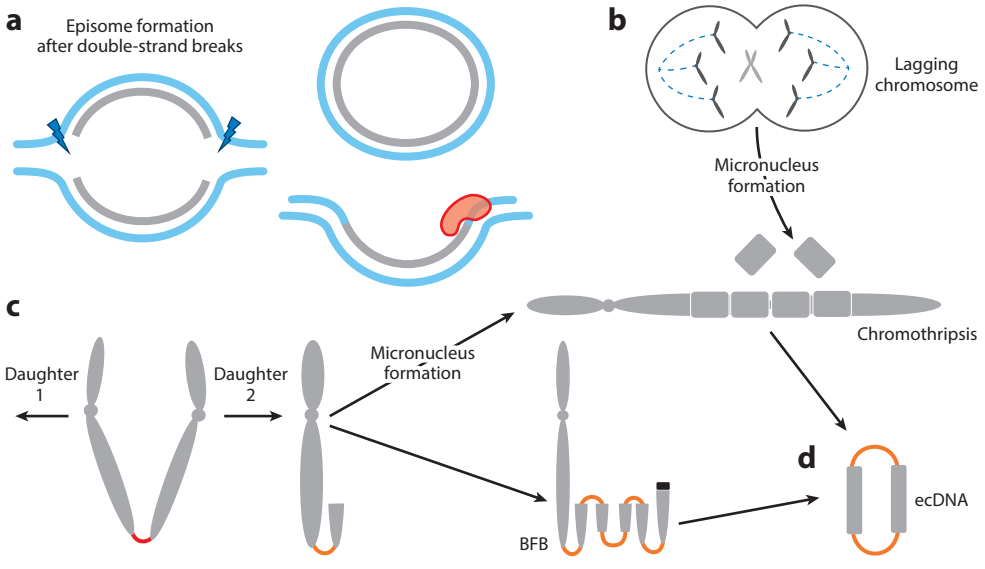

Figure 3

Mechanisms of ecDNA formation. (*a*) Episomes formed by replication fork stalling at a bubble, DNA breakage, and subsequent religation lead to ecDNA formation from one strand, while repair in the second strand allows replication to proceed without a deletion scar. (*b*) Missegregation errors may lead to a lagging chromosome followed by the formation of micronuclei. Shattering in subsequent mitoses and religation generate a chromothriptic chromosome. (*c*) Telomere loss and sister-chromatid bridging lead to broken ends or lagging chromosomes. Repeated BFB cycles may lead to a rearranged chromosome with an HSR-like signature. (*d*) ecDNA may form by fragments breaking off and circularizing during BFB cycles or chromothripsis. Abbreviations: BFB, breakage–fusion–bridge; ecDNA, extrachromosomal DNA; HSR, homogeneously staining region.

the initial excision, and therefore supported the postreplicative model. Storlazzi et al. (104) also identified strong structural similarities between ecDNA and HSR structures, indicating that the two modes of amplification share a common origin. The fusion of the two double-strand breaks was found to be mediated by nonhomologous end joining, a repair mechanism that is largely error free and can occur at all stages of the cell cycle (15, 70).

5.2. Chromothripsis

The rapid advent of genomic methods, including whole-genome sequencing, enabled ecDNA formation to be studied in the larger context of genome formation. Stephens et al. (102) observed extensive rearrangements, largely within a single chromosome of a patient with chronic lymphocytic leukemia. Moreover, the copy numbers on the chromosome followed a distinct oscillating pattern, suggesting a one-time, catastrophic shattering event they called chromothripsis. Subsequent work suggested that the formation of micronuclei is a critical event for chromothripsis occurrence (125). Mitotic errors can lead to missegregation of chromosomes and their physical isolation into aberrant micronuclear structures, and subsequent mitoses result in catastrophic shattering and recombination, or chromothripsis. Additionally, the rearranged by-products can include ecDNA, implicating chromothripsis as a source of ecDNA formation (61) (**Figure 3*b***). In an elegant confirmation of this idea, an experimental model of inducible Y chromosome centromere inactivation was used to generate a missegregation error that led to a lagging chromosome, the formation of micronuclei, and chromothripsis (61, 62). Whole-genome sequencing of clonally propagated rearrangements suggested extensive rearrangements and translocations consistent with chromothriptic breakage and religation, copy number changes, and ecDNA formation (60).

5.3. Breakage–Fusion–Bridge Cycles

The BFB cycle was first described by McClintock (68, 69) as a genomic abnormality in maize. A telomeric break leads to the formation of a chromatin bridge between sister chromatids during replication (**Figure 3*c***). When the sister chromatids are pulled apart during mitosis, an unequal cleavage might lead to a rearranged chromosome with a duplicated inversion at one end and a broken end that is rescued by bridge formation with a sister chromatid and a repeat of the BFB cycle (**Figure 3*d***). Lo et al. (55) suggested that the BFB cycle could result in genome instability and overexpression of oncogenes due to gene amplification. BFB-mediated rearrangements have often been described in explaining tumor genome arrangements, notably in the case of *HER2*-amplified breast cancers (65, 95). Umbreit et al. (109) utilized multiple experimental methods to induce telomere loss, including low-dose topoisomerase II inhibition and CRISPR-Cas9-mediated telomere loss on chromosome 4, allowing them to observe the consequence of bridge formation at high resolution. Telomere loss and bridge formation triggered a catastrophic sequence of events that could lead to extensive rearrangements and a chromothripsis-like signature. Specifically, the bridge formation occurred not only in sister chromatids but also among different chromosomes, resulting in multichromosomal rearrangement events. In parallel, the BFB cycle was shown to result in the breaking off and circularization of the rearranged fragments to form ecDNA (96), combining chromothripsis, BFB cycles, and ecDNA as part of a common smorgasbord of DNA instability.

5.4. Oncoviral Sequences Complete the Circle

Human papillomavirus (HPV) integration into the human genome in squamous cells of the cervix and oropharyngeal cavity is a major source of genome instability, and this integration is

associated with poor outcomes for patients (78). Analysis of the whole-genome data from HPV 16/18–positive cell lines revealed extensive rearrangements involving both viral and human sequences (2). Similar analyses of head and neck cancer samples suggested the presence of hybrid episomal structures (79). A reconstruction of the amplicon structures using HPV 16/18 reference genomes and the hg19 human genome assembly revealed the presence of hybrid ecDNA in nearly 50% of cervical cancer samples (22) and human-only or hybrid ecDNA in a third of head and neck cancer samples (81). ecDNA formation could be associated with increased expression of viral and human oncogenes, leading to increased genomic instability.

Taken together, these results suggest that ecDNA formation is a complex event and a consequence of compromised DNA damage repair that can occur through multiple distinct but nonexclusive rearrangement mechanisms. The initial event leading to ecDNA formation is likely to be stochastic, as analyses of breakpoints support nonhomologous end joining at junctions (62, 104). Even in ecDNAs that amplify the same oncogene, the exact breakpoints on either side of the oncogene are not conserved (43). Nevertheless, it is not understood whether the events are completely stochastic or have a tissue-specific bias. More experimental work is needed to clarify these and other missing facets of ecDNA formation.

6. FUNCTIONAL CHARACTERISTICS OF EXTRACHROMOSOMAL DNA

Selection is a key aspect of ecDNA maintenance in cells. Increased expression of oncogenes can increase the fitness of cancer cells in terms of growth and proliferation. Indeed, in a pan-cancer analysis, more than 50% of the oncogenes that showed >8× copy number amplification were found on ecDNA (43). Tissue specificity of ecDNA architecture has also been observed. An analysis of focal amplifications (and likely ecDNA) in the Cancer Genome Atlas data showed enrichment of *MDM4* and *EGFR* in glioblastoma, while breast cancer amplifications were enriched in *MYC* and *ERBB2* (22). Thus, while ecDNA formation might be stochastic, the tissue specificity of gene expression programs may lead to different selection pressures on an oncogene carrying ecDNA in different tissue types, resulting in a tissue-specific architecture. This explanation is not entirely satisfactory, however, because it suggests a high diversity of ecDNAs at formation, followed by selection-based pruning for specific ecDNAs. One possible explanation is that the formation of ecDNA, with respect to the location of double-strand breaks, is itself regulated, but the mechanisms for tissue-specific ecDNA formation remain to be elucidated.

6.1. Extrachromosomal DNA Chromatin Is Highly Accessible

An early study showed that ecDNAs carry accessible chromatin and that genes on ecDNAs are expressed, although not uniformly, providing a functional basis for selection (99). Initially, the overexpression was attributed entirely to the increase in copy number of the gene carried by the ecDNA. To test this idea, Wu et al. (118) used ATAC-seq (11, 18) and a related visual method, ATAC-see (17), to conduct a systematic assessment of chromatin accessibility in multiple cancer cell lines and primary tumor samples. The analysis revealed that ecDNAs contain among the most accessible chromatin in the cell and lack the higher-order conformation typical of heterochromatin, allowing for significantly higher levels of transcriptional activity (**Figure 4*a***). A large pan-cancer study of more than 3,000 samples showed a tremendous increase in expression of oncogenes on ecDNA relative to their expression on chromosomes, even after correcting for the increased copy number (43). Similarly, overexpression of the *NTF3* gene was observed in an ecDNA in a neuroblastoma sample, and its extrachromosomal origin was confirmed using allele-specific expression (44). These results emphasized how the unique architecture and epigenetics of

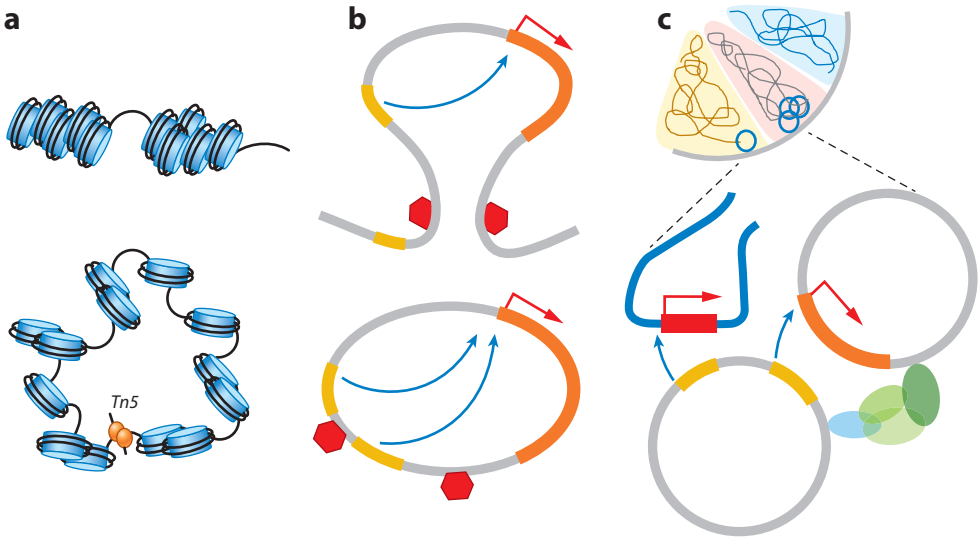

Figure 4

Functional characteristics of ecDNA. (*a*) In contrast to chromosomes (*top*), ecDNA (*bottom*) is highly accessible, resulting in overexpression of genes on ecDNA. The expression level remains high even after correcting for copy number. (*b*) TADs provide the regulatory elements that control gene regulation and shield the gene body from outside enhancers (*top*). The circular structure of ecDNA changes the regulatory circuitry through hijacking of enhancers outside the TAD (*bottom*). (*c*) ecDNAs form hubs and interact with chromosomes, resulting in enhancer activity that regulates genes in other ecDNAs and even on chromosomes. Abbreviations: ecDNA, extrachromosomal DNA; TAD, topologically associating domain.

ecDNA provide carrier cells with increased fitness, resulting in proliferation and increased tumor pathology.

6.2. Enhancer Hijacking

These results were rapidly extended in multiple directions, providing new insights into ecDNA biology. Chromatin capture technologies identify the spatial proximity of linearly distal regions of the chromosome, suggesting loop formation and topologically associating domains (TADs) that serve as boundaries of gene regulation (63). An independent circular chromosome conformation capture with high-throughput sequencing (4C-seq) experiment anchored on the *EGFR* promoter was used to interrogate glioblastoma samples and revealed a remarkable pattern (74, 118). In the sample where the *EGFR* copy number was not amplified, the expected strong contacts against known upstream enhancers were observed, and none were outside the 480-kb TAD that contained *EGFR* (**Figure 4*b***). However, in other samples, where *EGFR* was amplified on ecDNA, multiple new contacts were observed. The new contacts were outside the known TAD, suggesting a rewiring of the regulatory circuitry (74).

A similar experiment in neuroblastoma found that a *MYCN*-containing ecDNA connected distal regions of chromosome 2 into a single amplicon (33). Hi-C showed that enhancer-hijacking events connected enhancers in the distal region to the *n-Myc* promoter. The contact maps confirmed a new chromatin domain (neo-TAD formation) where "genes, enhancers, and insulators from distal parts of the genome" (33, p. 5) formed a novel, spatially interacting neighborhood. Nonconventional chromatin interactions have also been reported in medulloblastoma patients (16) and are likely to be a common feature of ecDNA gene regulation.

6.3. Regulatory *Trans*-Interactions

Remarkably, chromatin interaction analysis by paired-end tag sequencing (ChIA-PET) on glioblastoma-patient-derived neurosphere cell lines revealed that enhancer hijacking and regulatory rewiring are not limited to being within the ecDNA structure (126). Two cell lines, one carrying *c-Myc* and another carrying *EGFR*, showed extensive contacts not only within ecDNA but also between regions of ecDNA and other chromosomal regions (**Figure 4*c***). The contact sites on ecDNA and their chromosomal targets were enriched mostly at promoters. The ecDNA regions were enriched with marks of enhancer activity, including accessible chromatin and H3K27 acetylation, suggestive of regulatory function. Furthermore, transfection of artificial ecDNA into ecDNA-negative cell lines increased the activation of many chromosomal genes. Together, these results are suggestive of an "ecDNA party bus" (1) that brings a mobile enhancer to change the expression of chromosomal genes. The question remains whether these interactions are stochastic or recur in different cell types.

Aggregation of ecDNA had been observed previously but was generally assumed to be an aberrant condition suggestive of DNA damage in ecDNA, untethering of ecDNA from the chromosomes, and eviction of ecDNA via the formation of micronuclei (53). However, Hung et al. (36) observed a strong local concentration of the ecDNA FISH signal within the nuclei of many ecDNA-positive cancer cells, even though the signal arose from tens to hundreds of distinct ecDNA molecules. They suggested that hub formation was central to ecDNA biology. Live imaging showed that the hub formation was not static. During mitosis and in metaphase, the hubs separated into smaller particles and tethered to chromosomes. After mitosis, the hubs re-formed in the G1 phase. The authors also identified a bromodomain and extraterminal (BET) protein, Brd4, that was critical to hub maintenance. A BET inhibitor, JQ1, strongly and specifically disrupted ecDNA hubs. In the SNU-16 cell line, two distinct ecDNA molecules, one carrying *FGFR2* and the other carrying *Myc*, were found in the hubs. Enhancer elements on both ecDNAs cooperatively regulated *Myc*, thus establishing a novel instance of enhancer hijacking involving distinct ecDNAs. ecDNA hub formation was independently observed using a newly developed ecTag analysis technique (122). As the hubs dissociate in metaphase, hub formation is not inconsistent with random segregation. Inefficient dissociation could lead to nonrandom segregation and demand a revision of Equations 1 and 2. Note, however, that with clumped ecDNA, the segregation is more likely to be unequal, which would only exacerbate ecDNA-mediated pathology.

These results underscore the high accessibility of ecDNA chromatin and the dramatic reorganization of primary structure that results in the formation of new TADs and rewiring of the circuitry regulating genes on ecDNAs. Moreover, enhancers on ecDNAs can regulate distal genes on chromosomes or other ecDNAs that are proximal due to hub formation. The tremendous dysregulation of oncogenes achieved by ecDNA leads to the persistence of ecDNA due to a selective advantage, further leading to proliferation, increased pathology, and poor survival outcomes for patients whose tumor cells carry ecDNA (43).

7. THERAPY, EVOLUTION, RESISTANCE, AND FATE

The increased pathology of ecDNA-positive tumors underscores the need for intervention, while the unique biology of ecDNA raises hope of vulnerabilities specific to ecDNA. Identifying new targets and therapeutic intervention strategies is considered a "grand challenge" for cancer (25).

7.1. Extrachromosomal DNA Evolves and Adapts to Varying Selection Pressure

The early ecDNA research already pointed to the central role of ecDNA in tumor evolution and resistance. DHFR is an enzyme that reduces dihydrofolic acid to tetrahydrofolic acid, which is an

important component of multiple pathways of nucleotide synthesis. Methotrexate inhibits DHFR with a high affinity and is used as an anticancer agent. High doses of methotrexate were compensated by the formation of large numbers of ecDNAs carrying *DHFR* (10, 41, 42). The analysis also revealed mutations in *DHFR* that appeared during ecDNA formation and propagated with the increase in ecDNA copies (28, 29), although the functional characteristics of these mutations on ecDNA fitness have not been explored since those early results.

Somewhat surprisingly, continued treatment with methotrexate led to the integration of ecDNAs into HSRs as more stable structures with amplified copies of *DHFR* (42). Independently, Amler & Schwab (5) identified multiple tandem arrays of DNA segments containing the *n-Myc* oncogene in multiple neuroblastoma cell lines. They suggested a model involving spontaneous reintegration of (a single copy of) ecDNA followed by multiple tandem duplications. However, this model is less attractive because most observed ecDNA structures reveal conserved breakpoints down to the base-pair level (43). The multiple tandem duplication model would require that each tandem duplication event reuse the same breakpoints; however, despite considerable work in fragile site identification (26, 75), a correlation between ecDNA breakpoints and fragile sites has not been reported. We conjecture that a process comprising the aggregation of ecDNA into hubs (36), subsequent recombination into a larger structure, and a single integration event generates an HSR derived from ecDNA (**Figure 5**).

HSR formation also represents a mechanism of resistance. The SF295 cell line was shown to be ecDNA positive, with a gene encoding a G protein related to the family of ABC transporters, *ABCG2*, on ecDNA (86). At higher levels of dosage of the drug mitoxantrone, the number of ecDNAs decreased, but this was accompanied by a concomitant rise in HSRs, suggesting that the ecDNA had reintegrated into multiple nonnative chromosomal locations in response to treatment. Spectral karyotyping and FISH analysis showed evidence of integration of *ABCG2* along with a marked increase in structural variation (deletions, insertions, and translocations of genomic fragments) that were not apparent in the parental SF295 line prior to drug treatment.

Nathanson et al. (77) performed similar experiments in a glioblastoma cell line and found something remarkable. First, the cell line already carried *EGFRvIII*—a mutant of the receptor tyrosine kinase gene *EGFR*—on ecDNA, suggesting that ecDNA was a stable part of the maintenance of the cell line. Upon drug treatment with erlotinib, which targets EGFR, the ecDNA reintegrated into the chromosome as an HSR. The reintegration was concurrent with the arrival of a second

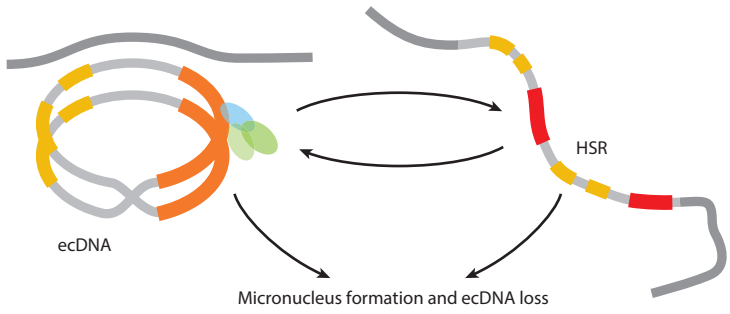

Figure 5

Plasticity of ecDNA and HSRs. Aggregated ecDNA can recombine into larger structures. Continued selection pressure that selects for amplification may lead to ecDNA formation, aggregation, and subsequent integration into a multicopy HSR. HSRs also show plasticity and change length. Removal of selection or DNA damage leads to the formation of micronuclei and loss of ecDNA. Abbreviations: ecDNA, extrachromosomal DNA; HSR, homogeneously staining region.

ecDNA species containing *FGFR2*. Although HSRs were considered to be a stable form of amplification, removal of the drug led to a reemergence of ecDNA carrying *EGFR*. Sequence-based analysis confirmed that the ecDNAs in the naive cells and those in the drug-removed cells had essentially identical structures, although with additional rearrangements in ecDNAs in the drug-removed cells (22, 77).

Recently, Song et al. (101) investigated the impact of BRAF and MEK inhibitors on a melanoma cell line carrying a mutant form of BRAF. The results provided another intriguing example of ecDNA-mediated drug resistance. With increasing drug dosage, an ecDNA arose that dramatically increased BRAF copy number. Over continued drug treatment, the ecDNA reintegrated into chromosome 3 in an aggregated HSR-like structure. Passage of the drug-addicted single-cell cloned cell line at low drug levels or in the absence of drug treatment resulted in a shortening or loss of the HSR. This result echoes some early observations on the plasticity of HSRs (9), but now demonstrating faster kinetics.

The above results are all consistent with the model represented by Equations 1 and 2 in a positive selection setting under the assumption that ecDNAs and HSRs are interconvertible states, although not functionally equivalent. More research is needed to clarify the functional differences between ecDNA and HSR states. The model also makes other simplifying assumptions—namely, that cells do not die and that ecDNAs are never lost. Thus, the impact of positive or negative selection is governed by a single parameter, s, which widens or narrows the distribution of ecDNAs among cells. While it is likely that the fitness of a tumor cell also depends on the number of ecDNAs, and not just on their presence or absence, more experimental data are needed to refine the model.

7.2. DNA Damage and Extrachromosomal DNA Loss

The role of the DNA damage sensing and repair system in the genesis and progression of ecDNA remains incompletely understood. ecDNA arises from a diversity of potential mechanisms, implicating different defects in DNA damage sensing and repair pathways. Furthermore, the DNA damage repair pathways engaged to promote ecDNA evolution once ecDNA has formed may differ from those involved in its inception. Consequently, there is a great deal about the link between DNA damage and ecDNA that remains to be discovered.

Snapka & Varshavsky (100) confirmed earlier findings that ecDNAs are lost once the methotrexate selection pressure is removed, over 25–30 cell doublings. As new ecDNAs are not being created, this effect could be explained simply by random drift without requiring negative selection. Remarkably, the authors also observed that low, noncytotoxic doses of hyroxyurea led to an acceleration of ecDNA loss, with 90% of the cells losing ecDNA in 4–5 doublings. These findings were later confirmed and extended to multiple cell lines and cytotoxic drugs (93, 114). Importantly, the loss of ecDNA was not mediated by inhibition of DNA synthesis; instead, the low doses of hydroxyurea were accompanied by an increase in the formation of micronuclei (**Figure 5**). These results were bolstered by a patient study that showed a slowing of progression in patients with advanced ovarian cancer upon treatment with low doses of hydroxyurea (87). Similarly, low doses of radiation were associated with a loss of *Myc*-carrying ecDNAs in a breast cancer cell line, primarily due to their entrapment in micronuclei (91).

The reduction in ecDNA upon cytotoxic drug treatment through the formation of micronuclei was recapitulated in other contexts (106). COLO320 DM lines, which had earlier been shown to be ecDNA positive (3), also lost ecDNA through the formation of micronuclei upon hydroxyurea treatment (94). Yu et al. (123) found that gemcitabine was similarly effective at greatly reduced doses for inducing the loss of ecDNA from the ovarian cancer cell line UACC-1598. As

an explanation, the authors proposed a mechanism in which cytotoxic drugs induce damage to ecDNAs, which break away from their chromosomal tethers. The lack of tethering leads to lagging of ecDNA aggregates during cell division, resulting in the formation of micronuclei enriched with ecDNA segments and the eventual eviction of ecDNA. Recent results suggest, however, that ecDNA aggregation (or hub formation) during interphase may be a natural part of ecDNA maintenance and not a consequence of DNA damage (36). The ecDNA hubs disaggregate during mitosis but are retained in the daughter nuclei by tethering to segregating chromosomes. For reasons that are not fully understood, DNA damage disrupts this process, leading to lagging aggregates of ecDNA and subsequent formation of micronuclei. The micronuclei may be lost in subsequent cell divisions or reintegrate into the nucleus, where they form larger ecDNAs and/or integrate into HSRs (80), possibly at locations with double-strand break lesions (96).

Poly(ADP-ribose) polymerase 1 (PARP1) is a central enzyme involved in many facets of DNA repair, including single-strand DNA breaks, nucleotide excision, and alternative nonhomologous end joining pathways. PARP inhibition, possibly in conjunction with other cytotoxic therapy, can accelerate DNA damage in cancer cells (97). It is particularly effective when homology-directed repair has been compromised, for example, through *BRCA* mutations (14). As sister chromatids are not available to ecDNA, it is possible that homology-directed repair is compromised, pointing to the viability of PARP inhibition for treating ecDNA-positive tumors. However, the integration of ecDNA into HSRs is also accelerated by PARP inhibitors, suggesting a possible mode of resistance (96), and due to the importance of nonhomologous end joining in ecDNA formation, DNA-dependent protein kinase catalytic subunit (DNA-PKcs) inhibitors reduce ecDNA formation (96). Future research aimed at understanding the role of DNA damage repair pathways in ecDNA maintenance is likely to be of high interest for targeting ecDNA (120).

8. CONCLUSION

The 23 pairs of chromosomes carry the instructions that make human life possible. The instructions are typically hidden and revealed only in tightly regulated settings to ensure that only the requisite type and amount of RNA—the precursor to the production of the molecular machinery—is expressed as needed for the cell to function in specific contexts. It is perhaps not surprising that much cellular machinery is dedicated to duplicating this information with high fidelity, so that each daughter cell receives nearly identical copies of the book of life, and to ensuring that the instructions are exposed at the right time and place.

We are reminded of the American architect Louis Sullivan, who coined the phrase "form follows function" to describe the principle that the shape of a building or object reflects its function or purpose. This phrase also aptly describes ecDNAs. First, their circular shape and lack of centromeres directly contribute to their nonchromosomal inheritance, and thus, the daughter cells do not receive the same book. Second, the instructions are highly accessible and their regulatory circuits are rewired, leading to a dysregulation of the expressed genes. It is likely that the dysregulation imposes negative fitness in general, leading to the rapid elimination of ecDNAs, which are therefore rarely seen in normal cells. However, in a few unfortunate instances, the extra copies of the gene (and an excess of gene products) provide a fitness advantage to the cells, which then proliferate at the expense of neighboring cells, leading to cancer. ecDNA-positive cancers adapt faster through a rapid change in the copy number of oncogenes, reveal novel resistance pathways, are less likely to mediate an immune response, and result in worse outcomes for patients. Finally, ecDNAs are prevalent, with a fifth to a third of all cancer samples being ecDNA positive.

New tools for investigating the shape and spatial organization of the genomes of ecDNA-containing cancers are providing unique insights into their biology. In that light, although ecDNAs

were discovered nearly 60 years ago, their prevalence in cancer and their central role in cancer pathogenicity are only just beginning to be appreciated.

DISCLOSURE STATEMENT

V.B. is a cofounder, consultant, and scientific advisory board member of and has equity interest in Boundless Bio Inc. and Abterra Biosciences Inc. The terms of this arrangement have been reviewed and approved by the University of California, San Diego, in accordance with its conflict-of-interest policies. P.S.M. is a cofounder of Boundless Bio Inc. and chairs its scientific advisory board, for which he is compensated.

ACKNOWLEDGMENTS

The authors thank an anonymous reviewer for many suggestions and corrections. V.B. was supported in part by grants from the National Institutes of Health (U24CA264379 and R01GM114362). P.S.M. was supported by grants from the National Brain Tumor Society and the National Institutes of Health (R01CA238349).

LITERATURE CITED

1. Adelman K, Martin BJE. 2021. ecDNA party bus: bringing the enhancer to you. *Mol. Cell* 81:1866–67
2. Akagi K, Li J, Broutian TR, Padilla-Nash H, Xiao W, et al. 2014. Genome-wide analysis of HPV integration in human cancers reveals recurrent, focal genomic instability. *Genome Res.* 24:185–99
3. Alitalo K, Schwab M, Lin CC, Varmus HE, Bishop JM. 1983. Homogeneously staining chromosomal regions contain amplified copies of an abundantly expressed cellular oncogene (c-*myc*) in malignant neuroendocrine cells from a human colon carcinoma. *PNAS* 80:1707–11
4. Alt FW, Kellems RE, Bertino JR, Schimke RT. 1978. Selective multiplication of dihydrofolate reductase genes in methotrexate-resistant variants of cultured murine cells. *J. Biol. Chem.* 253:1357–70
5. Amler LC, Schwab M. 1989. Amplified N-myc in human neuroblastoma cells is often arranged as clustered tandem repeats of differently recombined DNA. *Mol. Cell. Biol.* 9:4903–13
6. Balaban-Malenbaum G, Gilbert F. 1977. Double minute chromosomes and the homogeneously staining regions in chromosomes of a human neuroblastoma cell line. *Science* 198:739–41
7. Barker PE, Drwinga HL, Hittelman WN, Maddox AM. 1980. Double minutes replicate once during S phase of the cell cycle. *Exp. Cell Res.* 130:353–60
8. Beverley SM, Coderre JA, Santi DV, Schimke RT. 1984. Unstable DNA amplifications in methotrexate-resistant Leishmania consist of extrachromosomal circles which relocalize during stabilization. *Cell* 38:431–39
9. Biedler JL, Melera PW, Spengler BA. 1980. Specifically altered metaphase chromosomes in antifolate-resistant Chinese hamster cells that overproduce dihydrofolate reductase. *Cancer Genet. Cytogenet.* 2:47–60
10. Brown PC, Beverley SM, Schimke RT. 1981. Relationship of amplified dihydrofolate reductase genes to double minute chromosomes in unstably resistant mouse fibroblast cell lines. *Mol. Cell. Biol.* 1:1077–83
11. Buenrostro JD, Giresi PG, Zaba LC, Chang HY, Greenleaf WJ. 2013. Transposition of native chromatin for fast and sensitive epigenomic profiling of open chromatin, DNA-binding proteins and nucleosome position. *Nat. Methods* 10:1213–18
12. Cameron DL, Baber J, Shale C, Valle-Inclan JE, Besselink N, et al. 2021. GRIDSS2: comprehensive characterisation of somatic structural variation using single breakend variants and structural variant phasing. *Genome Biol.* 22:202
13. Carroll SM, DeRose ML, Gaudray P, Moore CM, Needham-Vandevanter DR, et al. 1988. Double minute chromosomes can be produced from precursors derived from a chromosomal deletion. *Mol. Cell. Biol.* 8:1525–33

14. Chang HY, Nuyten DSA, Sneddon JB, Hastie T, Tibshirani R, et al. 2005. Robustness, scalability, and integration of a wound-response gene expression signature in predicting breast cancer survival. *PNAS* 102:3738–43
15. Chang HY, Pannunzio NR, Adachi N, Lieber MR. 2017. Non-homologous DNA end joining and alternative pathways to double-strand break repair. *Nat. Rev. Mol. Cell Biol.* 18:495–506
16. Chapman OS, Luebeck J, Wani S, Tiwari A, Pagadala M, et al. 2021. The landscape of extrachromosomal circular DNA in medulloblastoma. bioRxiv 2021.10.18.464907. **https://doi.org/10.1101/2021.10.18.464907**
17. Chen X, Shen Y, Draper W, Buenrostro JD, Litzenburger U, et al. 2016. ATAC-see reveals the accessible genome by transposase-mediated imaging and sequencing. *Nat. Methods* 13:1013–20
18. Corces MR, Trevino AE, Hamilton EG, Greenside PG, Sinnott-Armstrong NA, et al. 2017. An improved ATAC-seq protocol reduces background and enables interrogation of frozen tissues. *Nat. Methods* 14:959–62
19. Cox D, Yuncken C, Spriggs AI. 1965. Minute chromatin bodies in malignant tumours of childhood. *Lancet* 286:55–58
20. Cross R. 2020. The curious DNA circles that make treating cancer so hard. *Chemical and Engineering News*, Oct. 18. **https://cen.acs.org/pharmaceuticals/oncology/curious-DNA-circles-make-treating/98/i40**
21. DeCarvalho AC, Kim H, Poisson LM, Winn ME, Mueller C, et al. 2018. Discordant inheritance of chromosomal and extrachromosomal DNA elements contributes to dynamic disease evolution in glioblastoma. *Nat. Genet.* 50:708–17
22. Deshpande V, Luebeck J, Nguyen NPD, Bakhtiari M, Turner KM, et al. 2019. Exploring the landscape of focal amplifications in cancer using AmpliconArchitect. *Nat. Commun.* 10:392
23. Evans GA. 1993. *Physical mapping of complex genomes*. US Patent 5,219,726
24. Fan Y, Mao R, Lv H, Xu J, Yan L, et al. 2011. Frequency of double minute chromosomes and combined cytogenetic abnormalities and their characteristics. *J. Appl. Genet.* 52:53–59
25. Foulkes I, Sharpless NE. 2021. Cancer grand challenges: embarking on a new era of discovery. *Cancer Discov.* 11:23–27
26. Fungtammasan A, Walsh E, Chiaromonte F, Eckert KA, Makova KD. 2012. A genome-wide analysis of common fragile sites: What features determine chromosomal instability in the human genome? *Genome Res.* 22:993–1005. Corrigendum. 2016. *Genome Res.* 26:1451
27. Garsed D, Marshall O, Corbin V, Hsu A, Di Stefano L, et al. 2014. The architecture and evolution of cancer neochromosomes. *Cancer Cell* 26:653–67
28. Haber DA, Beverley SM, Kiely ML, Schimke RT. 1981. Properties of an altered dihydrofolate reductase encoded by amplified genes in cultured mouse fibroblasts. *J. Biol. Chem.* 256:9501–10
29. Haber DA, Schimke RT. 1981. Unstable amplification of an altered dihydrofolate reductase gene associated with double-minute chromosomes. *Cell* 26:355–62
30. Hadi K, Yao X, Behr JM, Deshpande A, Xanthopoulakis C, et al. 2020. Distinct classes of complex structural variation uncovered across thousands of cancer genome graphs. *Cell* 183:197–210
31. Hahn PJ, Nevaldine B, Longo JA. 1992. Molecular structure and evolution of double-minute chromosomes in methotrexate-resistant cultured mouse cells. *Mol. Cell. Biol.* 12:2911–18
32. Hamkalo BA, Farnham PJ, Johnston R, Schimke RT. 1985. Ultrastructural features of minute chromosomes in a methotrexate-resistant mouse 3T3 cell line. *PNAS* 82:1126–30
33. Helmsauer K, Valieva ME, Ali S, Chamorro González R, Schöpflin R, et al. 2020. Enhancer hijacking determines extrachromosomal circular *MYCN* amplicon architecture in neuroblastoma. *Nat. Commun.* 11:5823
34. Hotta Y, Bassel A. 1965. Molecular size and circularity of DNA in cells of mammals and higher plants. *PNAS* 53:356–62
35. Hung K, Luebeck J, Dehkordi S, Coruh C, Law J, et al. 2021. Targeted profiling of human extrachromosomal DNA by CRISPR-CATCH. bioRxiv 2021.11.28.470285. **https://doi.org/10.1101/2021.11.28.470285**
36. Hung KL, Yost KE, Xie L, Shi Q, Helmsauer K, et al. 2021. ecDNA hubs drive cooperative intermolecular oncogene expression. *Nature* 600:731–36

37. Inazawa J, Abe T, Inoue K, Nishigaki H, Horiike S, et al. 1989. Simultaneous existence of double minute chromosomes and a homogeneously staining region in a retinoblastoma cell line (Y79) and amplification of N-myc at HSR. *Cancer Genet. Cytogenet.* 37:133–37
38. Int. Hum. Genome Seq. Consort. 2001. Initial sequencing and analysis of the human genome. *Nature* 409:860–921
39. Jaratlerdsiri W, Chan EKF, Petersen DC, Yang C, Croucher PI, et al. 2017. Next generation mapping reveals novel large genomic rearrangements in prostate cancer. *Oncotarget* 8:23588–602
40. Kanda T, Sullivan KF, Wahl GM. 1998. Histone-GFP fusion protein enables sensitive analysis of chromosome dynamics in living mammalian cells. *Curr. Biol.* 8:377–85
41. Kaufman RJ, Brown PC, Schimke RT. 1979. Amplified dihydrofolate reductase genes in unstably methotrexate-resistant cells are associated with double minute chromosomes. *PNAS* 76:5669–73
42. Kaufman RJ, Brown PC, Schimke RT. 1981. Loss and stabilization of amplified dihydrofolate reductase genes in mouse sarcoma S-180 cell lines. *Mol. Cell. Biol.* 1:1084–93
43. Kim H, Nguyen NP, Turner K, Wu S, Gujar AD, et al. 2020. Extrachromosomal DNA is associated with oncogene amplification and poor outcome across multiple cancers. *Nat. Genet.* 52:891–97
44. Koche RP, Rodriguez-Fos E, Helmsauer K, Burkert M, MacArthur IC, et al. 2020. Extrachromosomal circular DNA drives oncogenic genome remodeling in neuroblastoma. *Nat. Genet.* 52:29–34
45. Kohl NE, Kanda N, Schreck RR, Bruns G, Latt SA, et al. 1983. Transposition and amplification of oncogene-related sequences in human neuroblastomas. *Cell* 35:359–67
46. Koo DH, Molin WT, Saski CA, Jiang J, Putta K, et al. 2018. Extrachromosomal circular DNA-based amplification and transmission of herbicide resistance in crop weed *Amaranthus palmeri*. *PNAS* 115:3332–37
47. Kucheria K. 1968. Double minute chromatin bodies in a sub-ependymal glioma. *Br. J. Cancer* 22:696–97
48. Kumar P, Dillon LW, Shibata Y, Jazaeri AA, Jones DR, Dutta A. 2017. Normal and cancerous tissues release extrachromosomal circular DNA (eccDNA) into the circulation. *Mol. Cancer Res.* 15:1197–205
49. L'Abbate A, Macchia G, D'Addabbo P, Lonoce A, Tolomeo D, et al. 2014. Genomic organization and evolution of double minutes/homogeneously staining regions with *MYC* amplification in human cancer. *Nucleic Acids Res.* 42:9131–45
50. Lam ET, Hastie A, Lin C, Ehrlich D, Das SK, et al. 2012. Genome mapping on nanochannel arrays for structural variation analysis and sequence assembly. *Nat. Biotechnol.* 30:771–76
51. Lange JT, Chen CY, Pichugin Y, Xie L, Tang J, et al. 2022. Principles of ecDNA random inheritance drive rapid genome change and therapy resistance in human cancers. *Nat. Genet*. In press
52. Leung AK, Kwok TP, Wan R, Xiao M, Kwok PY, et al. 2017. OMBlast: alignment tool for optical mapping using a seed-and-extend approach. *Bioinformatics* 33:311–19
53. Levan A, Levan G. 1978. Have double minutes functioning centromeres? *Hereditas* 88:81–92
54. Li H, Durbin R. 2009. Fast and accurate short read alignment with Burrows-Wheeler transform. *Bioinformatics* 25:1754–60
55. Lo AW, Sabatier L, Fouladi B, Pottier G, Ricoul M, Murnane JP. 2002. DNA amplification by breakage/fusion/bridge cycles initiated by spontaneous telomere loss in a human cancer cell line. *Neoplasia* 4:531–38
56. Long J, Shelhamer E, Darrell T. 2015. Fully convolutional networks for semantic segmentation. In *2015 IEEE Conference on Computer Vision and Pattern Recognition*, pp. 3431–40. Piscataway, NJ: IEEE
57. Lubs HA, Salmon JH. 1965. The chromosomal complement of human solid tumors. II. Karyotypes of glial tumors. *J. Neurosurg.* 22:160–68
58. Luebeck J, Coruh C, Dehkordi SR, Lange JT, Turner KM, et al. 2020. AmpliconReconstructor integrates NGS and optical mapping to resolve the complex structures of focal amplifications. *Nat. Commun.* 11:4374
59. Lundberg G, Rosengren AH, Håkanson U, Stewénius H, Jin Y, et al. 2008. Binomial mitotic segregation of *MYCN*-carrying double minutes in neuroblastoma illustrates the role of randomness in oncogene amplification. *PLOS ONE* 3:e3099
60. Ly P, Brunner SF, Shoshani O, Kim DH, Lan W, et al. 2019. Chromosome segregation errors generate a diverse spectrum of simple and complex genomic rearrangements. *Nat. Genet.* 51:705–15
61. Ly P, Cleveland DW. 2017. Rebuilding chromosomes after catastrophe: emerging mechanisms of chromothripsis. *Trends Cell Biol.* 27:917–30

62. Ly P, Teitz LS, Kim DH, Shoshani O, Skaletsky H, et al. 2017. Selective Y centromere inactivation triggers chromosome shattering in micronuclei and repair by non-homologous end joining. *Nat. Cell Biol.* 19:68–75
63. Maass PG, Barutcu AR, Rinn JL. 2019. Interchromosomal interactions: a genomic love story of kissing chromosomes. *J. Cell Biol.* 218:27–38
64. Madhavi R, Guntur M, Ghosh R, Ghosh PK. 1990. Double minute chromosomes in the leukocytes of a young girl with breast carcinoma. *Cancer Genet. Cytogenet.* 44:203–7
65. Marotta M, Onodera T, Johnson J, Budd GT, Watanabe T, et al. 2017. Palindromic amplification of the *ERBB2* oncogene in primary HER2-positive breast tumors. *Sci. Rep.* 7:41921
66. Marshall OJ, Chueh AC, Wong LH, Choo KH. 2008. Neocentromeres: new insights into centromere structure, disease development, and karyotype evolution. *Am. J. Hum. Genet.* 82:261–82
67. McClintock B. 1932. A correlation of ring-shaped chromosomes with variegation in *Zea mays*. *PNAS* 18:672–81
68. McClintock B. 1939. The behavior in successive nuclear divisions of a chromosome broken at meiosis. *PNAS* 25:405–16
69. McClintock B. 1941. The stability of broken ends of chromosomes in *Zea mays*. *Genetics* 26:234–82
70. Meng X, Qi X, Guo H, Cai M, Li C, et al. 2015. Novel role for non-homologous end joining in the formation of double minutes in methotrexate-resistant colon cancer cells. *J. Med. Genet.* 52:135–44
71. Mitra AB, Murty VV, Luthra UK. 1983. Double-minute chromosomes in the leukocytes of a patient with a previous history of cervical carcinoma. *Cancer Genet. Cytogenet.* 8:117–22
72. Molin WT, Yaguchi A, Blenner M, Saski CA. 2020. The eccDNA replicon: a heritable, extranuclear vehicle that enables gene amplification and glyphosate resistance in *Amaranthus palmeri*. *Plant Cell* 32:2132–40
73. Møller HD, Lin L, Xiang X, Petersen TS, Huang J, et al. 2018. CRISPR-C: circularization of genes and chromosome by CRISPR in human cells. *Nucleic Acids Res.* 46:e131
74. Morton AR, Dogan-Artun N, Faber ZJ, MacLeod G, Bartels CF, et al. 2019. Functional enhancers shape extrachromosomal oncogene amplifications. *Cell* 179:1330–41.e13
75. Mrasek K, Schoder C, Teichmann AC, Behr K, Franze B, et al. 2010. Global screening and extended nomenclature for 230 aphidicolin-inducible fragile sites, including 61 yet unreported ones. *Int. J. Oncol.* 36:929–40
76. Müller HD. 2020. Circle-Seq: isolation and sequencing of chromosome-derived circular DNA elements in cells. *Methods Mol. Biol.* 2119:165–81
77. Nathanson DA, Gini B, Mottahedeh J, Visnyei K, Koga T, et al. 2014. Targeted therapy resistance mediated by dynamic regulation of extrachromosomal mutant EGFR DNA. *Science* 343:72–76
78. Nulton TJ, Kim NK, DiNardo LJ, Morgan IM, Windle B. 2018. Patients with integrated HPV16 in head and neck cancer show poor survival. *Oral Oncol.* 80:52–55
79. Nulton TJ, Olex AL, Dozmorov M, Morgan IM, Windle B. 2017. Analysis of The Cancer Genome Atlas sequencing data reveals novel properties of the human papillomavirus 16 genome in head and neck squamous cell carcinoma. *Oncotarget* 8:17684–99
80. Oobatake Y, Shimizu N. 2020. Double-strand breakage in the extrachromosomal double minutes triggers their aggregation in the nucleus, micronucleation, and morphological transformation. *Genes Chromosomes Cancer* 59:133–43
81. Pang J, Nguyen N, Luebeck J, Ball L, Finegersh A, et al. 2021. Extrachromosomal DNA in HPV-mediated oropharyngeal cancer drives diverse oncogene transcription. *Clin. Cancer Res.* 27:6772–86
82. Paulsen T, Malapati P, Shibata Y, Wilson B, Eki R, et al. 2021. MicroDNA levels are dependent on MMEJ, repressed by c-NHEJ pathway, and stimulated by DNA damage. *Nucleic Acids Res.* 49:11787–99
83. Paulsen T, Shibata Y, Kumar P, Dillon L, Dutta A. 2019. Small extrachromosomal circular DNAs, microDNA, produce short regulatory RNAs that suppress gene expression independent of canonical promoters. *Nucleic Acids Res.* 47:4586–96
84. Raeisi Dehkordi S, Luebeck J, Bafna V. 2021. FaNDOM: fast nested distance-based seeding of optical maps. *Patterns* 2:100248
85. Rajkumar U, Turner K, Luebeck J, Deshpande V, Chandraker M, et al. 2019. EcSeg: semantic segmentation of metaphase images containing extrachromosomal DNA. *iScience* 21:428–35

86. Rao VK, Wangsa D, Robey RW, Huff L, Honjo Y, et al. 2005. Characterization of *ABCG2* gene amplification manifesting as extrachromosomal DNA in mitoxantrone-selected SF295 human glioblastoma cells. *Cancer Genet. Cytogenet.* 160:126–33
87. Raymond E, Faivre S, Weiss G, McGill J, Davidson K, et al. 2001. Effects of hydroxyurea on extrachromosomal DNA in patients with advanced ovarian carcinomas. *Clin. Cancer Res.* 7:1171–80
88. Sachidanandam R, Weissman D, Schmidt SC, Kakol JM, Stein LD, et al. 2001. A map of human genome sequence variation containing 1.42 million single nucleotide polymorphisms. *Nature* 409:928–33
89. Sanborn JZ, Salama SR, Grifford M, Brennan CW, Mikkelsen T, et al. 2013. Double minute chromosomes in glioblastoma multiforme are revealed by precise reconstruction of oncogenic amplicons. *Cancer Res.* 73:6036–45
90. Scappaticci S, Fossati GS, Valenti L, Scabini M, Tateo S, et al. 1995. A search for double minute chromosomes in cultured lymphocytes from different types of tumors. *Cancer Genet. Cytogenet.* 82:50–53
91. Schoenlein PV, Barrett JT, Kulharya A, Dohn MR, Sanchez A, et al. 2003. Radiation therapy depletes extrachromosomally amplified drug resistance genes and oncogenes from tumor cells via micronuclear capture of episomes and double minute chromosomes. *Int. J. Radiat. Oncol. Biol. Phys.* 55:1051–65
92. Shale C, Baber J, Cameron DL, Wong M, Cowley MJ, et al. 2020. Unscrambling cancer genomes via integrated analysis of structural variation and copy number. bioRxiv 2020.12.03.410860. **https://doi.org/10.1101/2020.12.03.410860**
93. Shimizu N, Itoh N, Utiyama H, Wahl GM. 1998. Selective entrapment of extrachromosomally amplified DNA by nuclear budding and micronucleation during S phase. *J. Cell Biol.* 140:1307–20
94. Shimizu N, Misaka N, Utani K. 2007. Nonselective DNA damage induced by a replication inhibitor results in the selective elimination of extrachromosomal double minutes from human cancer cells. *Genes Chromosomes Cancer* 46:865–74
95. Shimizu N, Shingaki K, Kaneko-Sasaguri Y, Hashizume T, Kanda T. 2005. When, where and how the bridge breaks: Anaphase bridge breakage plays a crucial role in gene amplification and HSR generation. *Exp. Cell Res.* 302:233–43
96. Shoshani O, Brunner SF, Yaeger R, Ly P, Nechemia-Arbely Y, et al. 2021. Chromothripsis drives the evolution of gene amplification in cancer. *Nature* 591:137–41
97. Slade D. 2020. PARP and PARG inhibitors in cancer treatment. *Genes Dev.* 34:360–94
98. Smith CA, Vinograd J. 1972. Small polydisperse circular DNA of HeLa cells. *J. Mol. Biol.* 69:163–78
99. Smith G, Taylor-Kashton C, Dushnicky L, Symons S, Wright J, Mai S. 2003. c-Myc-induced extrachromosomal elements carry active chromatin. *Neoplasia* 5:110–20
100. Snapka RM, Varshavsky A. 1983. Loss of unstably amplified dihydrofolate reductase genes from mouse cells is greatly accelerated by hydroxyurea. *PNAS* 80:7533–37
101. Song K, Minami JK, Huang A, Dehkordi SR, Lomeli SH, et al. 2022. Plasticity of extrachromosomal and intrachromosomal *BRAF* amplifications in overcoming targeted therapy dosage challenges. *Cancer Discov.* 12:1046–69
102. Stephens PJ, Greenman CD, Fu B, Yang F, Bignell GR, et al. 2011. Massive genomic rearrangement acquired in a single catastrophic event during cancer development. *Cell* 144:27–40
103. Storlazzi CT, Fioretos T, Surace C, Lonoce A, Mastrorilli A, et al. 2006. MYC-containing double minutes in hematologic malignancies: evidence in favor of the episome model and exclusion of MYC as the target gene. *Hum. Mol. Genet.* 15:933–42
104. Storlazzi CT, Lonoce A, Guastadisegni MC, Trombetta D, D'Addabbo P, et al. 2010. Gene amplification as double minutes or homogeneously staining regions in solid tumors: origin and structure. *Genome Res.* 20:1198–206
105. Takayama S, Uwaike Y. 1988. Analysis of the replication mode of double minutes using the PCC technique combined with BrdUrd labeling. *Chromosoma* 97:198–203
106. Tanaka T, Shimizu N. 2000. Induced detachment of acentric chromatin from mitotic chromosomes leads to their cytoplasmic localization at G_1 and the micronucleation by lamin reorganization at S phase. *J. Cell Sci.* 113:697–707
107. Turner KM, Deshpande V, Beyter D, Koga T, Rusert J, et al. 2017. Extrachromosomal oncogene amplification drives tumour evolution and genetic heterogeneity. *Nature* 543:122–25

108. Tuzun E, Sharp AJ, Bailey JA, Kaul R, Morrison VA, et al. 2005. Fine-scale structural variation of the human genome. *Nat. Genet.* 37:727–32
109. Umbreit NT, Zhang CZ, Lynch LD, Blaine LJ, Cheng AM, et al. 2020. Mechanisms generating cancer genome complexity from a single cell division error. *Science* 368:eaba0712
110. Venter JC, Adams MD, Myers EW, Li PW, Mural RJ, et al. 2001. The sequence of the human genome. *Science* 291:1304–51
111. Vogt N, Gibaud A, Lemoine F, de la Grange P, Debatisse M, Malfoy B. 2014. Amplicon rearrangements during the extrachromosomal and intrachromosomal amplification process in a glioma. *Nucleic Acids Res.* 42:13194
112. Vogt N, Lefère SH, Apiou F, Dutrillaux AM, Cör A, et al. 2004. Molecular structure of double-minute chromosomes bearing amplified copies of the epidermal growth factor receptor gene in gliomas. *PNAS* 101:11368–73
113. Von Hoff DD, Forseth B, Clare CN, Hansen KL, VanDevanter D. 1990. Double minutes arise from circular extrachromosomal DNA intermediates which integrate into chromosomal sites in human HL-60 leukemia cells. *J. Clin. Investig.* 85:1887–95
114. Von Hoff DD, Waddelow T, Forseth B, Davidson K, Scott J, Wahl G. 1991. Hydroxyurea accelerates loss of extrachromosomally amplified genes from tumor cells. *Cancer Res.* 51:6273–79
115. Voullaire L, Saffery R, Davies J, Earle E, Kalitsis P, et al. 1999. Trisomy 20p resulting from inverted duplication and neocentromere formation. *Am. J. Med. Genet.* 85:403–8
116. Voullaire LE, Slater HR, Petrovic V, Choo KH. 1993. A functional marker centromere with no detectable alpha-satellite, satellite III, or CENP-B protein: activation of a latent centromere? *Am. J. Hum. Genet.* 52:1153–63
117. Wang Y, Wang M, Djekidel MN, Chen H, Liu D, et al. 2021. eccDNAs are apoptotic products with high innate immunostimulatory activity. *Nature* 599:308–14
118. Wu S, Turner KM, Nguyen N, Raviram R, Erb M, et al. 2019. Circular ecDNA promotes accessible chromatin and high oncogene expression. *Nature* 575:699–703
119. Xu K, Ding L, Chang TC, Shao Y, Chiang J, et al. 2019. Structure and evolution of double minutes in diagnosis and relapse brain tumors. *Acta Neuropathol.* 137:123–37
120. Yan Y, Guo G, Huang J, Gao M, Zhu Q, et al. 2020. Current understanding of extrachromosomal circular DNA in cancer pathogenesis and therapeutic resistance. *J. Hematol. Oncol.* 13:124
121. Yang L, Luquette LJ, Gehlenborg N, Xi R, Haseley PS, et al. 2013. Diverse mechanisms of somatic structural variations in human cancer genomes. *Cell* 153:919–29
122. Yi E, Gujar AD, Guthrie M, Kim H, Zhao D, et al. 2022. Live-cell imaging shows uneven segregation of extrachromosomal DNA elements and transcriptionally active extrachromosomal DNA hubs in cancer. *Cancer Discov.* 12:468–83
123. Yu L, Zhao Y, Quan C, Ji W, Zhu J, et al. 2013. Gemcitabine eliminates double minute chromosomes from human ovarian cancer cells. *PLOS ONE* 8:e71988
124. Zakov S, Kinsella M, Bafna V. 2013. An algorithmic approach for breakage-fusion-bridge detection in tumor genomes. *PNAS* 110:5546–51
125. Zhang CZ, Spektor A, Cornils H, Francis JM, Jackson EK, et al. 2015. Chromothripsis from DNA damage in micronuclei. *Nature* 522:179–84
126. Zhu Y, Gujar AD, Wong CH, Tjong H, Ngan CY, et al. 2021. Oncogenic extrachromosomal DNA functions as mobile enhancers to globally amplify chromosomal transcription. *Cancer Cell* 39:694–707